

Predicting Station-level Hourly Demands in a Large-scale Bike-sharing Network: A Graph Convolutional Neural Network Approach

Lei Lin, Zhengbing He, Srinivas Peeta, and Xuejin Wen

Abstract— Bike sharing is a vital piece in a modern multi-modal transportation system. However, it suffers from the bike unbalancing problem due to fluctuating spatial and temporal demands. Accurate bike sharing demand predictions can help operators to make optimal routes and schedules for bike redistributions, and therefore enhance the system efficiency. To the end, this study proposes a novel Graph Convolutional Neural Network with Data-driven Graph Filter (GCNN-DDGF) model to predict station-level hourly demands in a large-scale bike-sharing network. With each station as a vertex in the network, the new proposed GCNN-DDGF model is able to automatically learn the hidden correlations between stations, and thus overcomes a common issue reported in the previous studies, i.e., the quality and performance of GCNN models rely on the predefinition of the adjacency matrix. To show the performance of the proposed model, this study compares the GCNN-DDGF model with four GCNNs models, whose adjacency matrices are from different bike sharing system matrices including the Spatial Distance matrix (SD), the Demand matrix (DE), the Average Trip Duration matrix (ATD) and the Demand Correlation matrix (DC), respectively. The five types of GCNN models and the classic Support Vector Regression model are built on a Citi Bike dataset from New York City which includes 272 stations and over 28 million transactions from 2013 to 2016. Results show that the GCNN-DDGF model has the lowest Root Mean Square Error, followed by the GCNN-DC model, and the GCNN-ATD model has the worst performance. Through a further examination, we find the learned DDGF captures some similar information embedded in the SD, DE and DC matrices, and it also uncovers more hidden heterogeneous pairwise correlations between stations that are not revealed by any of those matrices.

Index Terms— Bike Sharing; Graph Convolution Neural Network; Data-driven Graph Filter; Deep Learning; Demand Prediction;

I. INTRODUCTION

A typical motorized passenger vehicle emits about 4.7 metric tons of carbon dioxide per year [1]. To decrease tailpipe emissions, reduce energy consumption and protect the

environment, as of December 2016, roughly 1,000 cities worldwide have started bike sharing programs [2]. Bike sharing can also help to solve the first mile and last mile problems [3], [4]. By providing a connection to other transportation modes, bike usage can seamlessly enable individual trips consisting of multiple transportation modes. Hence, bike sharing is becoming an important component of a modern, sustainable and efficient multi-modal transportation network.

In general, distributed bike sharing systems (BSSs) can be grouped into two types, dock-based BSS and non-dock BSS. In dock-based BSS, the bikes are rented from and returned to the docking stations. Examples of this BSS type can be found in US cities such as New York City, San Francisco, Chicago and Washington D.C. A non-dock BSS is designed to provide more freedom and flexibility to travelers in terms of access and bike usage. In contrast to dock-based BSS, riders are free to leave bikes wherever they want. Non-dock BSSs have been deployed in many cities in China by companies such as Ofo and Mobike this year, and have rapidly become a popular travel mode for travelers. By September 2017, there were 15 bike-sharing programs in operation in Beijing, China that deployed over 2.3 million bikes [5].

While bike sharing can greatly enhance urban mobility as a sustainable transportation mode, it has key limitations due to the effects of fluctuating spatial and temporal demand. As pointed out by many previous studies [6]–[8], it is common for BSSs with fixed stations that some stations are empty with no bikes to check out while others are full precluding bikes from being returned. For non-dock BSSs, enhanced flexibility poses even more challenges to ensure bike availability at some places and prevent surplus bikes from blocking sidewalks and parking areas. For both types of BSSs, accurate bike sharing demand predictions can help operators to make optimal routes and schedules for rebalancing to improve BSSs.

A lot of attention has been paid to the bike sharing demand prediction problem. Based on the focused spatial granularity, there are three groups of prediction models in literature: *city-level*, *cluster-level*, and *station-level*. For the city-level group, the object is to predict the bike usage for a whole city. In 2014,

Corresponding author: Srinivas Peeta.

L. Lin is with the NEXTRANS Center, Purdue University, West Lafayette, IN 47906 USA (e-mail: lin954@purdue.edu).

Z. He is with the School of Traffic and Transportation, Beijing Jiaotong University, Beijing, China.

S. Peeta is with the School of Civil Engineering, Purdue University, West Lafayette, IN 47906 USA, and also with the NEXTRANS Center, Purdue University, West Lafayette, IN 47906 USA (e-mail: peeta@purdue.edu).

Kaggle, the world largest platform for predictive modeling and analytics competitions, invited the participants to forecast the total hourly demand in the Capital Bike Share program in Washington, D.C. [9]. Giot and Cherrier (2014) made the demand predictions for next 24 hours with a city granularity for the Capital Bike Share system. They tested multiple machine learning algorithms such as Ridge Regression, Adaboost Regression, Support Vector Regression, Random Forest Tree and Gradient Boosting Regression Tree and showed the first two outperformed the others [10]. Although predicting the total city-level rentals from all the bike sharing stations simplifies the problem greatly, it doesn't contribute to solving the bike rebalancing among stations. More detailed transaction data collected by BSSs such as trip duration, origin, destination, check in/out time, user information and so on are not being fully utilized.

The assumption behind the cluster-level group is that some correlations exist among stations based on their geographical locations and temporal demands, and the total demands of these stations can be predicted as a cluster. For example, the bike usage patterns are usually similar for a small cluster of stations near a residential area in the morning rush hours. If the cluster-level predictions are accurate enough, one can always find an available bike within that cluster. A few studies have tried to identify these kinds of spatial-temporal clusters among stations. Zhou (2015) applied the Community Detection algorithm and the Agglomerative Hierarchical Clustering method to group the similar bike flows and stations in Chicago BSS. The paper verified that the bike usage patterns of the clusters are different by day, user, directional and land use profiles [7]. A few other studies have also applied clustering algorithms and then made the cluster-level bike sharing demand predictions. Li et al. (2015) proposed a bike sharing demand prediction framework that introduces a Bipartite Station Clustering algorithm to group individual stations. The whole city bike sharing demand is predicted based on Gradient Boosting Regression Tree and later split across clusters based on a Multi-similarity-based Inference model [6]. Chen et al. (2016) pointed out that the clustering of stations should be updated based on temporal and weather factors, social and traffic events. They proposed a Geographically-constrained station Clustering method over a weighted correlation network to dynamically group stations with similar bike usage patterns. Then they estimated the cluster-level rental and return numbers with the cluster's average value adjusted by an inflation rate [8]. More recently, Zhang et al. (2017) proposed an approach to partition a city into a grid map where each grid denotes a small region with size predefined. With the historical bike sharing demands for each grid known, the whole grid map can be transformed to an image through color coding. The accumulated image data are then used to train a Deep Spatial-temporal Residual Network. They showed that their model performs the best among a few traditional statistical models and deep learning models [11].

Station-level bike sharing demand prediction is more challenging [6], [8], and it has attracted considerable interest. Rixey (2013) built linear regression models for predicting monthly rentals by station in three BSSs Capital Bike Share,

Denver B-Cycle, and Nice Ride MN systems. Independent variables such as demographic factors and built environment factors are extracted based on a 400-meter buffer around each station [12]. Faghih-Imani et al. (2014) built similar linear mixed models to predict the hourly bike sharing demand by station based on a two-day dataset for BIXI bicycle sharing system in Montreal. Similarly, a 250-meter buffer is set up for each station to generate explanatory variables in the model [13]. These two studies don't consider any underlying correlations among stations, e.g., one bike station near subway exit has high demands during peak-hour, another one close to it may also have high demands. Yang et al. (2016) proposed a probabilistic mobility model which considers the previous check-out records and trip durations to estimate the future check-in numbers at each station [14]. However, for bicycle check-out or demand predictions, they applied the Random Forest tree algorithm for each isolated station without leveraging the spatial or temporal correlations between stations.

Given considerable bike sharing data in a large network, this study is interested in utilizing the underlying correlations between stations to predict the hourly demand per-station with deep learning techniques. Deep learning models have been popular in the past few years, and one main reason is that they can extract useful features from raw data through multiple-layer neural network learning. The training of deep learning models requires big data and can be accomplished with the development of high-performance computation tools such as Graphics Processing Unit (GPU). Convolutional Neural Network (CNN), which is one type of state-of-the-art deep learning models, is able to successfully extract highly meaningful statistical patterns and learn local stationary structures presented in data such as image and video. CNN can identify similar features with localized filters or kernels, and these shift-invariant filters are learned from data and able to recognize identical features independently of their spatial locations [15]. However, CNN is only defined and can be applied straightforwardly for data domain with regular grids such as images. For data lying on irregular or non-Euclidean domains such as user data on social networks and gene data on biological regulatory networks, the graph has been applied as a main structure to encode the heterogeneous pairwise correlations and complex geometric structures in data [15].

Recently some emerging studies have aimed at generalizing CNN for graph-structured data. One approach is to utilize the signal processing theory on graphs [16]–[18]. Given an undirected and connected graph, each vertex has a signal or feature vector, and an adjacency matrix (weighted or binary) is defined where each entry encodes the degree of relation between signal vectors at two vertices [18]. The Laplacian matrix [17] or the adjacent matrix [18] of the graph can be decomposed to form the Fourier basis. The Graph Fourier Transform is then performed to convert the signal data from vertex domain to frequency domain. Then graph spectral filtering can be easily conducted to amplify or attenuate the contributions of some of the components [17]. Defferrard et al. (2016) proposed a fast localized spectral filtering approach and applied their GCNN model on text classification and showed

the results are promising [15]. Kipf and Welling (2016) applied a similar localized spectral filter, which is further simplified with the first-order approximation. Multiple citation datasets were used to test their GCNN for semi-supervised learning, and their approach outperforms the other related models in both efficiency and accuracy [19]. However, as pointed out by the authors, the main GCNN shortcoming is that one needs to create the graph artificially, predefine the adjacency matrix, and the quality of the input graph is of paramount importance [15], [20].

In this study, we propose a novel deep learning model Graph Convolutional Neural Network with data-driven graph filter (GCNN-DDGF) model for this station-level hourly demand prediction task. The proposed GCNN-DDGF model doesn't require the predefinition of the adjacency matrix, and thus can learn the hidden correlations between stations automatically. For comparison, four GCNNs are also built based on a bike sharing graph with stations as vertices and adjacency matrix predefined from one of the following BSS matrices including the Spatial Distance matrix (SD), the Demand matrix (DE), the Average Trip Duration matrix (ATD) and the Demand Correlation matrix (DC). The five types of GCNN models as well as the benchmark model Support Vector Regression (SVR) are built on a dataset from Citi BSS at New York City, which includes 272 stations and over 28 million transactions from 2013 to 2016. To the best of our knowledge, this is the first time that deep learning approach is applied for station-level hourly demand prediction for such a large-scale BSS. The results show that the learned DDGF can uncover more underlying correlations between stations than the predefined adjacency matrices and the novel GCNN-DDGF model has the lowest Root Mean Square Error (RMSE).

The rest of the paper is organized as follows. The methodology of the GCNN model is presented in detail in next section, including the predefinition of four types of adjacency matrices and the DDGF approach. The dataset from the Citi BSS is then introduced, so are the data preprocessing procedures. The following section compares the prediction performances of the models and explicitly analyzes the learned DDGF. The conclusion and future research directions are summarized at last.

II. METHODOLOGY

This section first describes GCNN and spectral filtering methodology. After that, multiple approaches to define the adjacency matrix in a bike sharing network are discussed. Our data-driven approach to learn the graph spectral filter is then introduced.

A. Graph Convolutional Neural Network

Suppose we have a graph $G = (V, x, \mathcal{E}, A)$, where V is a finite set of vertices with size N , a signal $x \in \mathbb{R}^N$ means a scalar for every vertex. \mathcal{E} is a set of edges, $A \in \mathbb{R}^{N \times N}$ is the adjacency matrix, and the entry A_{ij} encodes the connection degree between the signals at two vertices. A normalized graph Laplacian matrix is defined as

$$L = I_N - D^{-1/2} A D^{-1/2} \quad (1)$$

where I_N is the identity matrix; $D \in \mathbb{R}^{N \times N}$ is the diagonal degree matrix with $D_{ii} = \sum_j A_{ij}$.

L is a real symmetric positive semidefinite matrix which can be diagonalized as

$$L = U \Lambda U^T \quad (2)$$

where $U = [u_0, u_1, \dots, u_{N-1}]$; $\Lambda = \text{diag}([\lambda_0, \lambda_1, \dots, \lambda_{N-1}])$; $\lambda_0, \lambda_1, \dots, \lambda_{N-1}$ are the eigenvalues of L and u_0, u_1, \dots, u_{N-1} are the corresponding set of orthonormal eigenvectors.

1) Graph Fourier Transform and Spectral Filtering

Analogous to the Fourier transform which is the expansion of a signal in terms of the complex exponentials, the graph Fourier transform is defined as the expansion of a signal in terms of the eigenvectors of the graph Laplacian [17]:

$$\hat{x} = U^T x \quad (3)$$

Furthermore, the graph spectral filtering is defined as:

$$\hat{x}_{out} = g_\theta(\Lambda) \hat{x} \quad (4)$$

where $g_\theta(\Lambda)$ is a function of the eigenvalues of L .

A form of polynomial filters have been used in a few studies [15], [17], [19]:

$$g_\theta(\Lambda) = \sum_{k=0}^K \theta_k \Lambda^k \quad (5)$$

where $\theta \in \mathbb{R}^K$ is a vector of polynomial coefficients.

Then the inverse graph Fourier transform is given by

$$x_{out} = U \hat{x}_{out} \quad (6)$$

Finally merging (3)-(6), a spectral convolution on the graph is defined as follows:

$$g_\theta * x = U g_\theta(\Lambda) U^T x = \sum_{k=0}^K \theta_k U \Lambda^k U^T x = \sum_{k=0}^K \theta_k L^k x \quad (7)$$

where $L^k = (U \Lambda U^T)^k = U \Lambda^k U^T$.

Hammond et al. (2011) shows that the entry $(L^k)_{i,j} = 0$ when the shortest path distance between vertices i and j is greater than k [21]. Therefore this type of filter is also known as K -localized filter. The physical meaning of the graph spectral convolution is it combines the signal at the central vertex with the signals at vertices that are maximum K steps away.

To improve the computation efficiency, Kipf and Welling (2016) simplified the calculation of $g_\theta * x$ by just using the first-order polynomial [19]:

$$g_\theta * x \approx \theta_0 x + \theta_1 \tilde{L} x \quad (8)$$

where \tilde{L} is a rescaled Laplacian matrix, $\tilde{L} = \frac{2}{\lambda_{max}} L - I_N$, λ_{max} is the maximum eigenvalue of L .

Furthermore, Kipf and Welling (2016) approximately set $\lambda_{max} = 2$ since the neural network parameters will adapt to this change in scale during training,

$$g_\theta * x \approx \theta_0 x + \theta_1 (L - I_N) x \quad (9)$$

Replace L with (1),

$$g_\theta * x \approx \theta_0 x - \theta_1 D^{-\frac{1}{2}} A D^{-\frac{1}{2}} x \quad (10)$$

To constrain the number of parameters to further reduce the overfitting risk, let $\theta' = \theta_0 = -\theta_1$,

$$g_\theta * x \approx \theta' (I_N + D^{-\frac{1}{2}} A D^{-\frac{1}{2}}) x \quad (11)$$

When applied to the multi-layer structure, renormalization is applied at each layer to retain numerical stability:

$$I_N + D^{-\frac{1}{2}} A D^{-\frac{1}{2}} \rightarrow \tilde{D}^{-\frac{1}{2}} \tilde{A} \tilde{D}^{-\frac{1}{2}} \quad (12)$$

where $\tilde{A} = A + I_N$ is the summation of the adjacency matrix of the undirected graph A and the identity matrix I_N . In another word, \tilde{A} considers the self-connections; $\tilde{D}_{ii} = \sum_j \tilde{A}_{ij}$.

Generalize this convolution calculation to a signal $X \in \mathbb{R}^{N \times C}$ where each vertex v_i has a C -dimensional feature vector X_i ,

$$Z = \tilde{D}^{-\frac{1}{2}} \tilde{A} \tilde{D}^{-\frac{1}{2}} X \Theta \quad (13)$$

where $\Theta \in \mathbb{R}^{C \times F}$ is a matrix of filter parameters; $Z \in \mathbb{R}^{N \times F}$ is the convolved signal matrix.

2) Layer-wise Calculation

Suppose GCNN model has layers from 0, 1, ... to m from the input to the output. For each layer l , $l = 1, \dots, m-1$, the GCNN model $f(X, A)$ propagates from the input to the output with the following rule:

$$H^l = \sigma(Z^{l-1} W_T^l) = \sigma\left(\tilde{D}^{-\frac{1}{2}} \tilde{A} \tilde{D}^{-\frac{1}{2}} H^{l-1} \Theta^{l-1} W_T^l\right) \quad (14)$$

where Z^{l-1} is the convolved signal matrix in the $(l-1)^{th}$ layer; $W_T^l \in \mathbb{R}^{F^{l-1} \times C^l}$ is a layer-specific trainable weight matrix; $\sigma(\cdot)$ is an activation function, in this study, we apply $ReLU(\cdot) = \max(0, \cdot)$; $H^l \in \mathbb{R}^{N \times C^l}$ is the matrix of activations in the l^{th} layer, $H^0 = X$.

The product of $\Theta^{l-1} \in \mathbb{R}^{C^{l-1} \times F^{l-1}}$ and $W_T^l \in \mathbb{R}^{F^{l-1} \times C^l}$ can be learned by the neural network as one matrix $W^l \in \mathbb{R}^{C^{l-1} \times C^l}$, therefore (13) can be simplified as:

$$H^l = \sigma\left(\tilde{D}^{-\frac{1}{2}} \tilde{A} \tilde{D}^{-\frac{1}{2}} H^{l-1} W^l\right) \quad (15)$$

For the output layer m , the result is:

$$H^m = \tilde{D}^{-\frac{1}{2}} \tilde{A} \tilde{D}^{-\frac{1}{2}} H^{m-1} W^m \quad (16)$$

where $W^m \in \mathbb{R}^{C^{m-1} \times C^m}$ are the weight parameters to be learned; $H^m \in \mathbb{R}^{N \times C^m}$ are the predictions, e.g., the bike sharing demands of the N stations for the next hour when $C^m = 1$.

B. Graph Filter for Bike Sharing Demand Prediction

GCNN model relies on the structure of the graph. The adjacent matrix \tilde{A} needs to be defined first, with which the graph spectral filter can be approximated. This section lists four typical matrices in a BSS to quantify the correlations between stations. Correspondingly, four types of adjacent matrices \tilde{A} can be constructed.

1) Spatial Distance Matrix

The first natural way to encode the connection between stations is simply through the spatial distance [17]. The spatial distance (SD) matrix can be built through the spherical distances with the latitudes and longitudes of the stations known. If two stations are spatially close to each other, they are connected in the bike sharing graph network, the element of \tilde{A} is then defined as:

$$\tilde{A}_{ij} = \begin{cases} 1 & \text{if } DIST_{ij} \leq \kappa_{SD} \\ 0 & \text{if } DIST_{ij} > \kappa_{SD} \end{cases} \quad (17)$$

where $DIST_{ij}$ is the spherical distance between station i and j ; κ_{SD} is a predefined SD threshold.

2) Demand Matrix

This approach makes use of the check in and check out station information in the bike sharing transaction records. The symmetric demand matrix (DE), which considers the total demands between station i and j , is built as following:

$$DE_{ij} = \begin{cases} OD_{ij} + OD_{ji} & \text{if } i \neq j \\ OD_{ij} & \text{otherwise} \end{cases} \quad (18)$$

where OD_{ij} are the aggregated demands from station i to station j .

For this bike sharing graph network, if high demands exist between two stations, they are connected. A threshold parameter κ_{DE} is set to build a binary \tilde{A} that $\tilde{A}_{ij} = 1$ if $DE_{ij} \geq \kappa_{DE}$, otherwise let $\tilde{A}_{ij} = 0$.

3) Average Trip Duration Matrix

This approach utilizes the trip duration information in the bike sharing transaction records on the basis of DE matrix. Each entry ATD_{ij} in an Average Trip Duration matrix (ATD) is defined as:

$$ATD_{ij} = TTD_{ij} / DE_{ij} \quad (19)$$

where TTD_{ij} is the total trip durations of all the trips between station i and j ; DE_{ij} is the entry in the DE matrix.

Similarly, a binary adjacent matrix is formed that $\tilde{A}_{ij} = 1$ if $ATD_{ij} \leq \kappa_{ATD}$, otherwise let $\tilde{A}_{ij} = 0$. κ_{ATD} is a pre-defined threshold. In another word, the bike sharing graph network based on the ATD matrix is to connect two stations if the average trip duration between them are short.

4) Demand Correlation Matrix

This approach tries to capture the temporal demand correlations between stations by employing the check-out times of the bike sharing transaction records. The Demand Correlation matrix (DC) is defined by calculating the Pearson Correlation Coefficient (PCC) based on a pair of hourly bike demand series from stations.

$$DC_{ij} = PCC(h_i, h_j) \quad (20)$$

where h_i and h_j are the hourly bike demand series from station i and j .

In this approach, the bike sharing graph network is made by connecting two stations with high PCC; each entry of \tilde{A} is further set to 1 if $DC_{ij} \geq \kappa_{DC}$, otherwise let $\tilde{A}_{ij} = 0$; κ_{DC} is the DC threshold.

C. Data-Driven Graph Filter

The predefinition of the adjacency matrix \tilde{A} is not trivial. The hidden correlations between stations may be heterogeneous, therefore it may be hard to encode them using just one kind of metrics such as the SD, DE, ATD or DC matrix. Now suppose the adjacency matrix \tilde{A} is unknown, let $\hat{A} = \tilde{D}^{-\frac{1}{2}} \tilde{A} \tilde{D}^{-\frac{1}{2}}$, (15) becomes:

$$H^l = \sigma(\hat{A} H^{l-1} W^l) \quad (21)$$

where \hat{A} is a symmetric matrix consisting of trainable filter parameters.

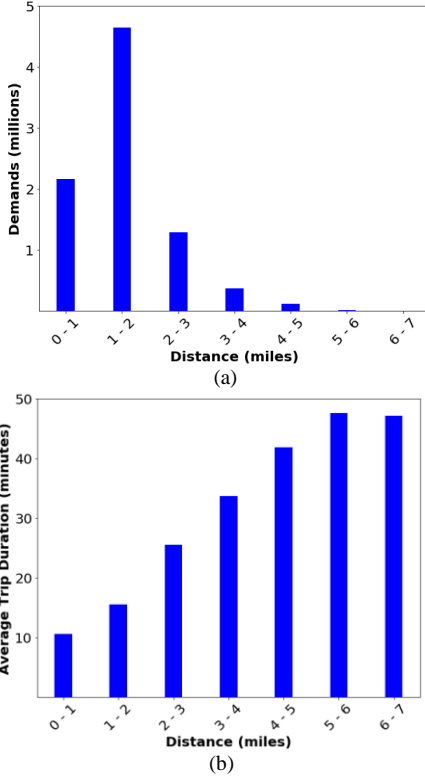


Fig. 3 (a) Aggregated Demands between Stations by Distance; (b) Average Trip Durations by Distance.

Fig. 3(a) shows the aggregated demands between stations by distance based on the DE and SD matrices. The highest demands are over 4.5 million trips when the distance between stations is 1 to 2 miles. The demands drop when the distance is too close (0 to 1 mile), and become lower and lower when the distance is farther. The average trip durations by distance based on the ATD and SD are shown in Fig. 3(b). The average duration is about 10 minutes for the trips within 1 mile. It increases with the distance and can take more than 45 minutes when the trips are longer than 5 miles. Note that the actual trip distances are unknown, and here it is the spherical distance based on the latitudes and longitudes of stations.

The 272×272 entries in the DC matrix which are the Pearson correlation coefficients between stations are shown in Fig. 4(a). The temporal bike demands of the stations are highly correlated. Fig. 4(b) further shows the normalized histogram of the demand correlation coefficients. There are no coefficients negative. The majority part looks like a Gaussian distribution with mean equal to 0.50. There are also 0.5% of correlation coefficients pretty close to 1.

IV. MODEL DEVELOPMENT AND RESULTS

Suppose the bike sharing demands of all the stations at hour i are $x_i \in \mathbb{R}^N$, $N = 272$, using the demands from the previous $(C^0 - 1)$ hours, we can construct a feature matrix $X_i \in \mathbb{R}^{N \times C^0}$, $X_i = [x_{i-C^0+1}, \dots, x_i]$ and the corresponding target vector $y_i \in \mathbb{R}^N$, the bike sharing demands of all the stations at the next hour. The original training dataset is transferred into records $\{(X_i, y_i)\}$, $i = C^0, \dots, 22,304$. The selection of C^0 will be

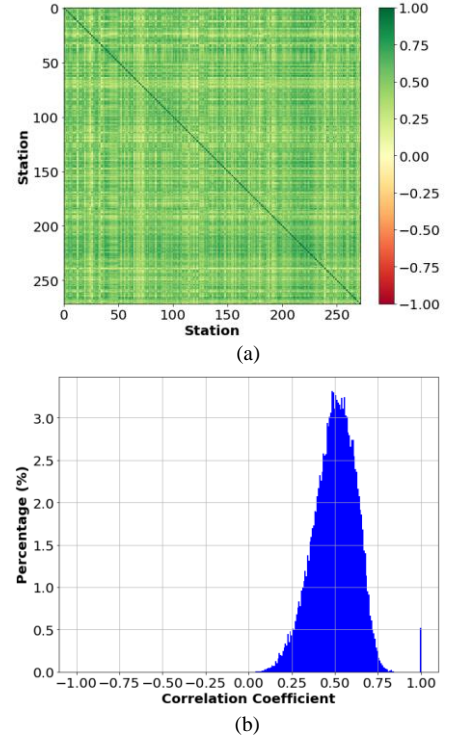


Fig. 4 (a) Visualization of the DC Matrix; (b) Normalized Histogram of Demand Correlation Coefficients

described later. In total we build five types of GCNN models, GCNN-SD, GCNN-DE, GCNN-ATD, GCNN-DC and GCNN-DDGF, which are named based on how the adjacency matrix is generated. To evaluate the performances, Root Mean Square Error (RMSE) is taken as the main criterion:

$$RMSE = \sqrt{\frac{1}{M \cdot N} \sum_i^M \sum_j^N (P_{ij} - y_{ij})^2} \quad (22)$$

where M is the dataset size; P_{ij} and y_{ij} are the predicted and recorded bike demands at hour i for station j .

A. Hyper-parameter Selection for GCNN models

In machine learning, hyper-parameters are parameters whose values are set prior to the commencement of the learning process [23]. The traditional way of performing hyper-parameter optimization is grid search, which is to manually specify the subset of hyper-parameter space and perform the search exhaustively. The trained model is evaluated on the validation dataset to determine the optimal hyper-parameters.

TABLE 1 summarizes the hyper-parameters in GCNN models. For each parameter, we use *start:step:end* to define the searching space, e.g., 1:2:5 represents the space $\{1, 3, 5\}$. The first group of hyper-parameters are used to determine the architecture of GCNN models. They include the threshold th to form the adjacency matrix from the SD, DE, ATD or DC matrix and the feature vector length at the input layer C^0 and those at the hidden layer 1 and 2: C^1 and C^2 . Note that we only considered the GCNNs with at most two hidden layers in this study; if C^2 is 0, it means the optimal model only needs one hidden layer. The second group includes two parameters learning rate α and mini-batch size B in the classic Stochastic Gradient Descent Algorithm (SGD). The third group is to

prevent overfitting. Overfitting means the model is fitting random errors or noises instead of the underlying relationship. With early stopping mechanism, the training algorithm terminates when the performance on validation dataset hasn't improved for a pre-specified threshold of iterations s . The stored best model on the validation dataset is returned as the final model.

TABLE 1
HYPER-PARAMETER SELECTION IN GCNN MODELS

| Hyper-parameters | GCNN Models | | | | | |
|------------------|-------------|-------|--------------|------------------|-------------|----|
| | SD | DE | ATD | DC | DD | GF |
| Model | th | 1:2:5 | 500:200:1100 | 10:10:30 | 0.5:0.2:0.9 | NA |
| Architecture | C^0 | | | 24:12:36 | | |
| | C^1 | | | 20:20:40 | | |
| | C^2 | | | 0:20:40 | | |
| SGD | α | | | 0.005:0.005:0.01 | | |
| | B | | | 100:100:200 | | |
| Over-fitting | s | | | 20:10:30 | | |

Based on TABLE 1, the experiments are conducted using Python 3.0 in Ubuntu 16.04 Linux System with 64 GB RAM and GTX 1080 Graphics Card. The models are developed using TensorFlow, an open-source deep learning neural network library maintained by Google [24]. TensorFlow supports GTX 1080 GPU which provides strong computation power. The optimal hyper-parameters are listed in TABLE 2. For all GCNN models, setting more than one hidden layer doesn't improve the performances, and the hyper-parameters except th are almost the same.

TABLE 2
OPTIMAL HYPER-PARAMETERS AND PERFORMANCE ON VALIDATION DATASET

| | | GCNN Models | | | | |
|----------------------------|----------|-------------|------|------|-------|-------------|
| | | SD | DE | ATD | DC | DDGF |
| Optimal Hyper-parameters | th | 3 | 900 | 20 | 0.9 | NA |
| | C^0 | 36 | 24 | 36 | 24 | 24 |
| | C^1 | 40 | 40 | 40 | 40 | 40 |
| | C^2 | 0 | 0 | 0 | 0 | 0 |
| | α | 0.01 | 0.01 | 0.01 | 0.005 | 0.005 |
| | B | 100 | 100 | 100 | 100 | 100 |
| | s | 20 | 20 | 20 | 20 | 20 |
| RMSE on Validation Dataset | | 3.39 | 3.36 | 3.97 | 3.14 | 2.97 |

For the performances on validation dataset, GCNN-DDGF learns the optimal graph filter \hat{A} directly from the data, its RMSE on validation dataset is only 2.97. In contrast, the RMSE of GCNN-DC is 3.14 when only the stations with highly correlated hourly demand series are connected in the graph (the threshold κ_{DC} is set as high as 0.9). The GCNN-SD and GCNN-DE have the validation RMSEs as 3.39 and 3.36 separately, and the GCNN-ATD performs the worst with the validation RMSE as 3.97. It's worth pointing out that we also construct the graphs with weighted adjacency matrices, which means that the entries in the SD, DE, ATD or DC are directly set as the edge weights in the graphs if they satisfy the threshold requirements, but unexceptionally the performances of GCNNs based on these graphs are worse than the GCNNs on graphs with binary adjacency matrices. This verifies the previous studies that the

adjacent matrix is of paramount importance [15], [20] for GCNN models, and pre-define the correlations between stations in a reasonable way is not trivial.

B. Model Comparison on Testing Dataset

Except for the five GCNN models, the benchmark model Support Vector Regression (SVR) is developed based on the scikit-learn package [25] in Python. SVR models have been applied widely in short-term traffic flow prediction [26], [27]. However, for SVR with nonlinear Kernels, it is hard to scale to a dataset with more than 10,000 samples [28]. In this study, the SVR with Radial Basis Function Kernel is tried but never completes the training. Instead, we apply the linear SVR, which greatly reduces the training time. Grid search is also applied to tune the SVR model. The penalty parameter is set as 1, and the Epsilon parameter is set as 0.5. Finally, the performances of all the six models on the testing dataset are compared in Fig. 5..

For the testing dataset GCNN-DDGF has the lowest RMSE as 2.35. GCNN-DC is the second best, and the following are GCNN-DE, SVR and GCNN-SD respectively. With all the others having RMSE less than 3, GCNN-ATD has the worst RMSE 3.44, which indicates the ATD is not appropriate as the graph adjacency matrix. The station RMSEs of all the six models are also compared in Fig. 5.. The stations are sorted based on their RMSEs given by GCNN-DDGF model, which are in the range of around 1 and more than 6. For all the models, the station with the largest RMSE is "Pershing Square North". Again, it is obvious that GCNN-DDGF and GCNN-DC have relatively lower station RMSEs comparing with the other models.

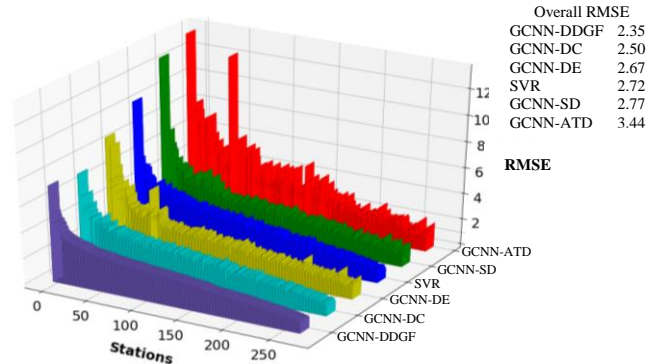


Fig. 5. Model Comparison on Testing Dataset

C. Graph Network Analysis based on DDGF

A bike sharing network can be built by taking the learned DDGF \hat{A} as the adjacency matrix. This graph network is visualized and analyzed using the popular tool Gephi [29]. Fig. 6(a) is the network visualization under the Geolocation layout in Gephi that the positions of the bike stations are determined by their latitude and longitude coordinates; and Fig. 6(b) is the visualization with Force Atlas layout which tries to avoid vertex overlapping. It's worth noting a few points as follows for better understanding of the visualizations. For the edges, the DDGF \hat{A} is normalized that all the entries fall within $[0, 1]$. Only 1,565 edges with weights not less than 0.15 are kept, and the edge thickness is proportional to its weight. With respect to the

vertices, the vertex size is proportional to the Weighted Degree (WD), which is the weight sum of its edges including the self-connected one. Each vertex is labeled with its station name. Furthermore, the visualizations in Fig. 6. denote eight large communities with different colors. These communities are generated using the modularity optimization algorithm [7], [30], [31]. Simply putting, the modularity measures the strength of a network partition. It is maximized when the network is divided into clusters with vertices connected densely, but for the vertices belonging to different clusters they are sparsely connected. The sizes of these communities are also labeled, e.g., “Community 1-55” means there are 55 stations in Community 1. In total there are 251 out of 272 stations in these communities.

Fig. 6(a) shows that the communities have various shapes spatially. While the stations in Community 1 mainly scatter in the middle part of Manhattan, some stations within the same community may scatter far from each other. For example, station “Central Park S & 6 Ave” in the north and station “West St & Chamber St” in the south are both in Community 2. However, the spherical distance between the two stations is as far as 6.1 miles. The stations in Community 7 locate along the Lafayette Street, which is a major north-south street in New York City's Lower Manhattan. Fig. 6(b) shows the edge weight strength is generally stronger within the same community, e.g., Community 2 and 4. The vertices with the top two largest WDs are station “Pershing Square North” and station “Grand Army Plaza & Central Park S”. As can be seen, these two stations are connected with quite a few other stations.

1) Weighted Degree Analysis

WD is one of the most important measurements in graph analysis. It is interesting to understand what factors may impact the WDs in the bike sharing graph from the DDGF. Fig. 7(a) explores the correlations between WD and total demands per station in the training dataset. The linear regression model is

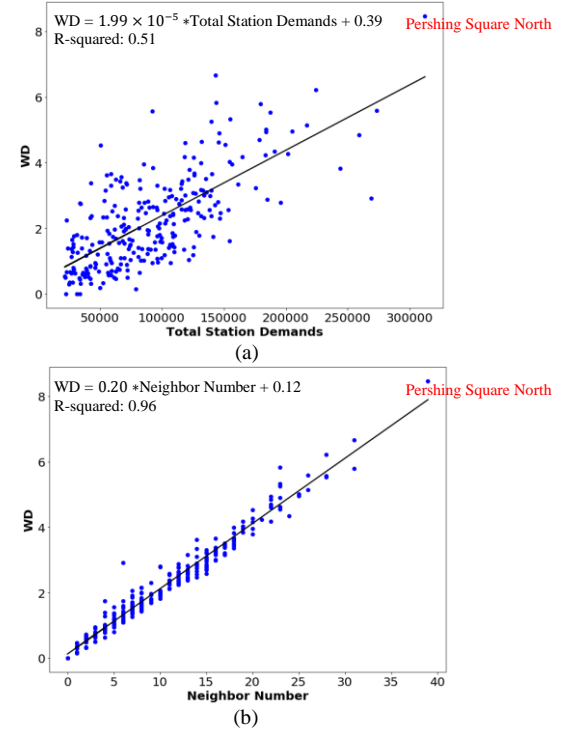


Fig. 7 (a) Linear Regression between WD and Total Station Demand; and (b) Linear Regression between WD and Neighbor Number.

applied to fit the points. It shows that in general WD is larger when the total demands of the station are higher. The R squared value of the linear regression model is 0.51. Station “Pershing Square North” has the highest total demands over 300,000 and the largest WD 8.46. Similarly, for each vertex in the bike sharing graph from the DDGF, the number of neighbors connecting with it can also be calculated. Fig. 7(b) plots the points based on WD and the neighbor number. It shows higher WD means this vertex has more neighbors, and the linear regression model fits the data points very well with R squared value 0.96. Station “Pershing Square North” has the largest WD

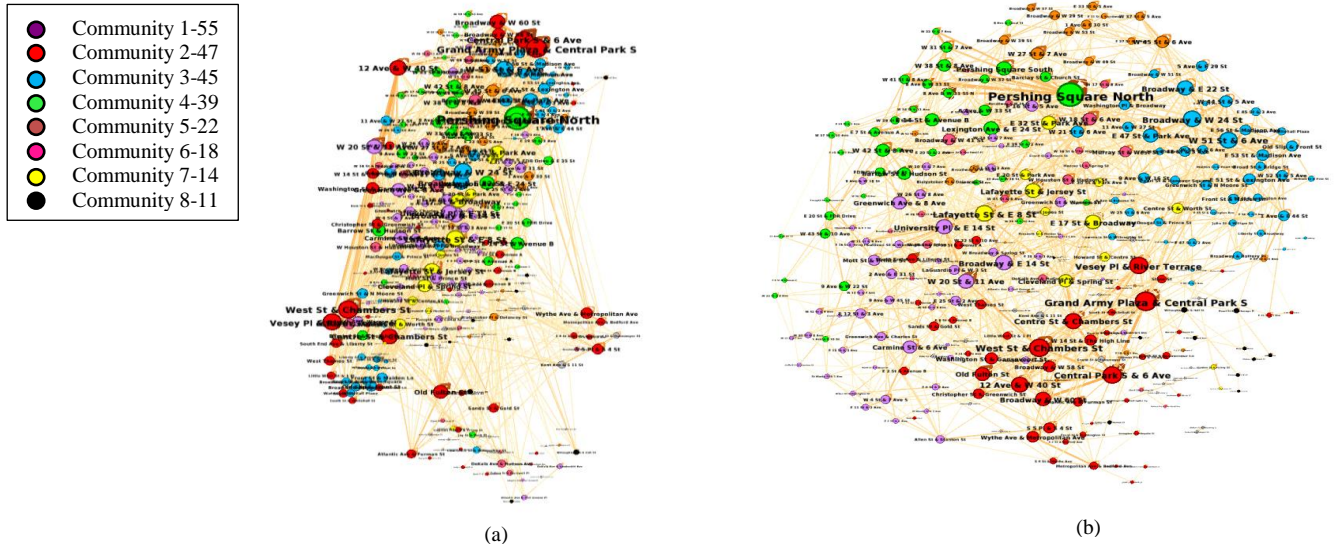


Fig. 6 (a) Visualization of the Bike Sharing Network based on DDGF - Geolocation Layout; and (b) Visualization of the Bike Sharing Network based on DDGF - Force Atlas Layout

and as more as 39 neighbors. One previous study mentioned Station “Pershing Square North” is the most popular station in Citi BSS because of its convenient access to NYC’s major transit hub Grand Central Terminal for commuters [32]. The largest WD and high neighbor number indicate the DDGF tries to gather information from more stations to improve the hourly demand predictions for it.

Fig. 8(a) continues to apply the linear regression with station RMSE as the dependent variable and WD as the explanatory variable. It shows that station RMSE increases with the increase of WD in general. Higher WD means it’s more difficult to predict the demands for that station and results in higher RMSE. Two stations “Pershing Square North” and “Duffield St & Willoughby St” are picked out. The former has the largest WD, and the latter has the smallest one. Fig. 8(b) and Fig. 8(c) compare one week (06/19/2016 – 06/25/2016) of predictions with real values for these two stations.

As can be seen, Station “Pershing Square North” is much busier with the highest hourly demand close to 120, which is only 10 for station “Duffield St & Willoughby St”. Station “Pershing Square North” is more difficult to predict, e.g., the real values are extremely larger than the predictions during the peak hour periods such as the afternoons on Tuesday, Wednesday, and Saturday.

2) Comparison between DDGF and Other Matrices

We are interested to compare the learned DDGF with the other matrices like the SD, DE, and DC to figure out why GCNN-DDGF performs better than the other GCNNs. The ATD matrix is not considered because GCNN-ATD has much worse performance on the testing dataset.

In Fig. 9., for each of the eight communities in the bike sharing graph from DDGF, the average of the edge weights is calculated by the distance between stations. It verifies that the spatial shapes of the communities are different as shown in Fig. 6(a), e.g., the farthest distance between stations in Community 7 is only 2-3 miles, but for Community 2 and 6, the longest one could be 5-6 miles. For all the communities, the average edge weight is the largest when the stations are spatially close to each other (0-1 miles); after that, the average edge weight curves have a large drop when the distance changes to 1-2 miles. Then the curves almost keep steady for Community 1, 3 and 6.

However, there also exist some fluctuations for a few communities, for example, for Community 2 and 4, the average edge weight becomes relatively higher again when it is 3-4 miles. To some extent the DDGF is like the SD; the demands at one station have connections mainly with its spatially close neighbors; e.g., the bike demands are usually similar for a few stations near the subway in the morning rush hours. However, the DDGF also reveals that the edge weight could still be large when the two stations are far from each other. Therefore the DDGF covers more heterogeneous pairwise information than the SD matrix.

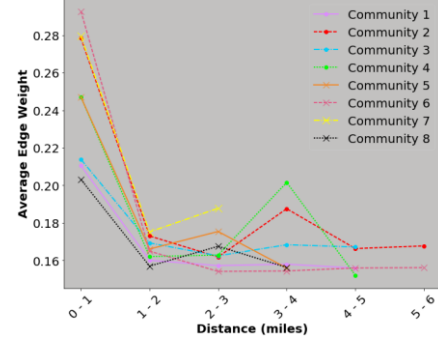


Fig. 9. Average Edge Weight by Spatial Distance

To unveil whether the learned DDGF \hat{A} can also capture some information from the DE and DC matrices, we pick the stations with the top four largest WDs “Pershing Square North”, “Grand Army Plaza & Central Park S”, “West St & Chambers St”, and “Central Park S & 6 Ave”. For each station, the corresponding row in \hat{A} is sorted from the largest to the lowest to rank its neighbors including the itself. As shown in each subplot of Fig. 10., the first column are those neighbors that have the top 10 largest edge weights, and the ranks are marked. The ranks of these neighbors based on the DE and DC matrices are also shown in the second and third columns. For convenience, the station square is colored as green if its rank is in the top 10 list; otherwise, the color is set as red.

Fig. 10. shows that first for each station, it’s always the self-connection that has the largest edge weight, which reveals its own demand series plays the most important role in predicting the next hour demand. Another observation may explain why station “Central Park S & 6 Ave” in the north and station “West

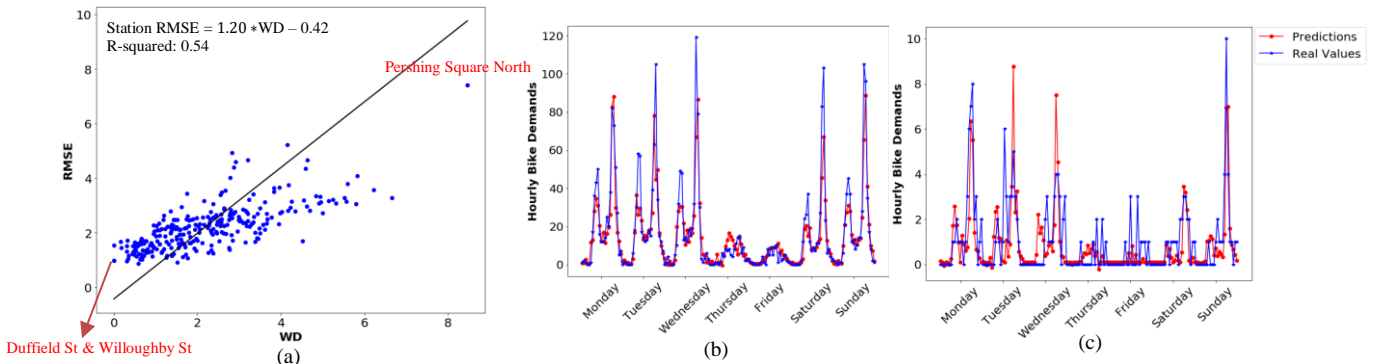


Fig. 8 (a) Linear Regression between Station RMSE and WD; (b) Predictions and Real Values for “Pershing Square North” (06/19/2016 – 06/25/2016); and (c) Predictions and Real Values for “Duffield St & Willoughby St” (06/19/2016 – 06/25/2016)

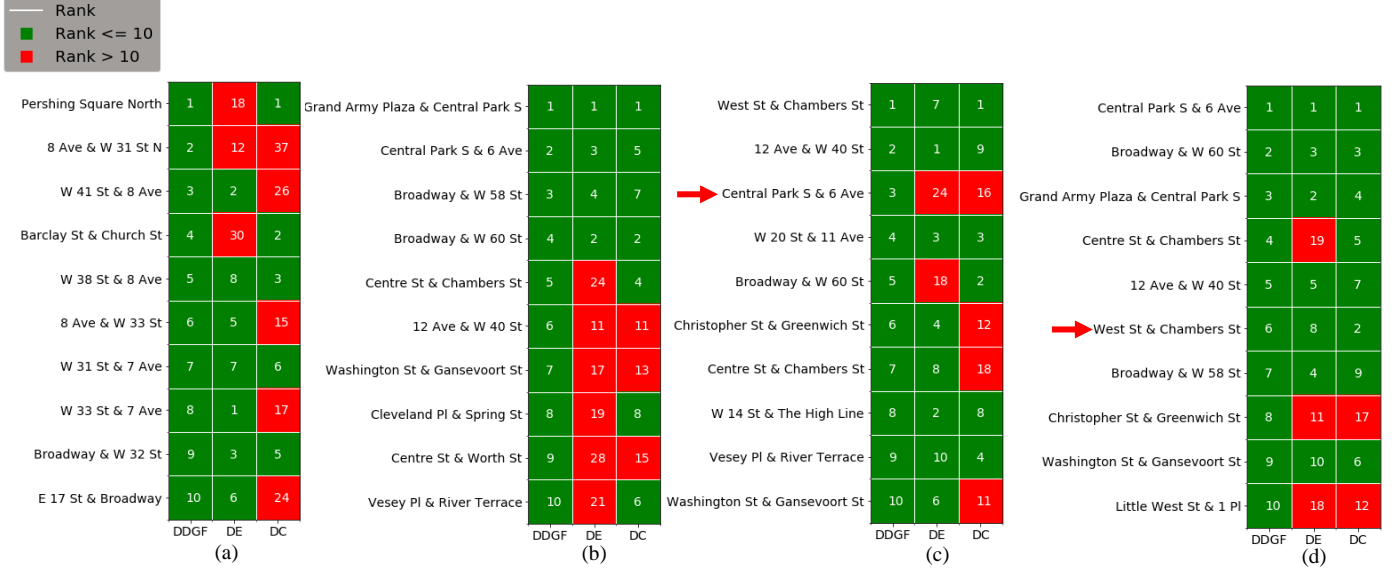


Fig. 10. Ranks of Neighbors for Stations with Top Four Highest WDs (a) Pershing Square North; (b) Grand Army Plaza & Central Park S; (c) West St & Chambers St; and (d) Central Park S & 6 Ave

St & Chamber St” in the south are strongly connected in Fig. 6.. As shown in Fig. 10(d), for station “Central Park S & 6 Ave”, “West St & Chamber St” is ranked 6th based on the DDGF, 8th based on the DC matrix, and 2nd based on the DE matrix. This tells that the demand series of “West St & Chamber St” can definitely help to predict the next hour demand of station “Central Park S & 6 Ave”. For station “West St & Chamber St” in Fig. 10(c), the edge weight between it and “Central Park S & 6 Ave” is ranked 3rd among its neighbors, but the other two ranks based DE and DC are only 24th and 16th separately. This may indicate that the relationship between the two stations is not simply symmetric. As a future research direction, GCNN-DDGF should be extended to the directed graph so that the edge weights between stations can cover distinct connections.

Finally, in Fig. 10. most of the times the squares are green that the ranks based on the learned DDGF, DE, and DC are consistent. Take station “Central Park S & 6 Ave” in Fig. 10(d) as an example, for the neighbor stations in the top 10 rank based on the DDGF, 7 of them are also in the top 10 lists based on the DE and DC. However, sometimes the ranking based on the DDGF may not agree with that from either DE or DC matrix. For example, for station “Grand Army Plaza & Central Park S” in Fig. 10(b), the neighbors from rank 5 to 10 based on the DDGF have much lower ranks from the DE matrix, and 3 out of them are also not in the top 10 list based on the DC matrix. Like the conclusion from Fig. 9., this shows the DDGF does include some information in the DE and DC matrices although none of them are used as the inputs of the GCNN-DDGF algorithm; at the same time, the DDGF also encodes some hidden connections between stations that cannot be explained by the DE and DC matrices.

V. CONCLUSION AND FUTURE RESEARCH DIRECTION

The paper proposes a novel GCNN-DDGF model for station-level hourly demand prediction in a large-scale bike-sharing network. Different from the state-of-the-art CNN model, the GCNN-DDGF model doesn’t require the data to have regular grid structure like images. Instead, it can deal with the situation when the data are embedded in a graph network, e.g., the bike sharing network. The spectral graph convolution for data at vertices includes graph Fourier Transform, filtering and inverse graph Fourier Transform three operations. To improve the computation efficiency, one localized first-order approximation of spectral graph convolution is through the normalized adjacency matrix considering self-connections. The proposed GCNN-DDGF model can deal with the main issue of GCNN that its performance relies on the predefined graph structure. For comparison, this paper considers GCNNs with adjacency matrices built from multiple BSS matrices such as the SD, DE, ATD, and DC matrices. The five types of GCNN models and another benchmark model SVR are built on a dataset from New York City Citi BSS which includes over 28 million transactions from 2013 to 2016. The bike-sharing graph network based on the learned DDGF is analyzed in detail. Some main conclusions are as follows:

- The GCNN-DDGF has the lowest RMSE among the six models, followed by the GCNN-DC, and the GCNN-ATD is much worse than the other models. It verifies the previous studies that the performance of GCNN model depends heavily on the predefined structure of the graph. In contrast the GCNN-DDGF can capture the heterogeneous pairwise correlations automatically to improve the predictions.
- The vertex WD is positively correlated with the total station demand and neighbor number. In general, higher WD means it’s more difficult to predict the

demand for that station and it may result in a higher station RMSE;

- For the communities in the bike sharing graph with the learned DDGF, the average edge weight is the largest when the spatial distance between stations is 0-1 miles; it has an obvious decreasing trend with the increase of the distance, but later it may either keep steady or fluctuate. For the stations with top four largest WDs, the ranks of the neighbors based on the DDGF are consistent with the ranks from the DE and DC matrices most of the time. However, some exceptions also exist. It indicates although none of the SD, DE and DC matrices are used as the inputs of the GCNN-DDGF, the DDGF does capture some similar information, furthermore the DDGF also uncover the hidden correlations among stations that are not revealed by the SD, DE or DC matrices.

In the future, it is interesting to import more variables such as the weather and social events (holidays and sports games) into the bike sharing demand prediction models. The current model can be improved to an online model which can adjust the hyper-parameters continuously. The GCNN models can also be applied to solve other transportation problems represented by the graphs such as subway station demand prediction, network traffic state estimation and so on. Finally, it is also interesting to make the model to learn a sparse graph filter and applicable to a directed graph.

REFERENCES

- [1] O. US EPA, "Greenhouse Gas Emissions from a Typical Passenger Vehicle," *US EPA*, 12-Jan-2016. [Online]. Available: <https://www.epa.gov/greenvehicles/greenhouse-gas-emissions-typical-passenger-vehicle-0>. [Accessed: 16-Oct-2017].
- [2] "List of bicycle-sharing systems," *Wikipedia*. 15-Oct-2017.
- [3] J.-R. Lin, T.-H. Yang, and Y.-C. Chang, "A hub location inventory model for bicycle sharing system design: Formulation and solution," *Comput. Ind. Eng.*, vol. 65, no. 1, pp. 77–86, May 2013.
- [4] J. Zhao, J. Wang, and W. Deng, "Exploring bikesharing travel time and trip chain by gender and day of the week," *Transp. Res. Part C Emerg. Technol.*, vol. 58, no. Part B, pp. 251–264, Sep. 2015.
- [5] "Over 2.5 Million Bikes in Beijing Bike Sharing Systems." [Online]. Available: <http://tech.sina.com.cn/i/2017-09-07/docifykuffc4167998.shtml>. [Accessed: 16-Oct-2017].
- [6] Y. Li, Y. Zheng, H. Zhang, and L. Chen, "Traffic Prediction in a Bike-sharing System," in *Proceedings of the 23rd SIGSPATIAL International Conference on Advances in Geographic Information Systems*, New York, NY, USA, 2015, p. 33:1–33:10.
- [7] X. Zhou, "Understanding Spatiotemporal Patterns of Biking Behavior by Analyzing Massive Bike Sharing Data in Chicago," *PLOS ONE*, vol. 10, no. 10, p. e0137922, Oct. 2015.
- [8] L. Chen *et al.*, "Dynamic Cluster-based Over-demand Prediction in Bike Sharing Systems," in *Proceedings of the 2016 ACM International Joint Conference on Pervasive and Ubiquitous Computing*, New York, NY, USA, 2016, pp. 841–852.
- [9] "Bike Sharing Demand." [Online]. Available: <https://www.kaggle.com/c/bike-sharing-demand>. [Accessed: 16-Oct-2017].
- [10] R. Giot and R. Cherrier, "Predicting bikeshare system usage up to one day ahead," in *2014 IEEE Symposium on Computational Intelligence in Vehicles and Transportation Systems (CIVTS)*, 2014, pp. 22–29.
- [11] J. Zhang, Y. Zheng, and D. Qi, "Deep Spatio-Temporal Residual Networks for Citywide Crowd Flows Prediction," in *Thirty-First AAAI Conference on Artificial Intelligence*, 2017.
- [12] R. Rixey, "Station-Level Forecasting of Bikesharing Ridership," *Transp. Res. Rec. J. Transp. Res. Board*, vol. 2387, pp. 46–55, Dec. 2013.
- [13] A. Faghih-Imani, N. Eluru, A. M. El-Geneidy, M. Rabbat, and U. Haq, "How land-use and urban form impact bicycle flows: evidence from the bicycle-sharing system (BIXI) in Montreal," *J. Transp. Geogr.*, vol. 41, no. Supplement C, pp. 306–314, Dec. 2014.
- [14] Z. Yang, J. Hu, Y. Shu, P. Cheng, J. Chen, and T. Moscibroda, "Mobility Modeling and Prediction in Bike-Sharing Systems," in *Proceedings of the 14th Annual International Conference on Mobile Systems, Applications, and Services*, New York, NY, USA, 2016, pp. 165–178.
- [15] M. Defferrard, X. Bresson, and P. Vandergheynst, "Convolutional Neural Networks on Graphs with Fast Localized Spectral Filtering," in *Advances in Neural Information Processing Systems 29*, D. D. Lee, M. Sugiyama, U. V. Luxburg, I. Guyon, and R. Garnett, Eds. Curran Associates, Inc., 2016, pp. 3844–3852.
- [16] J. Bruna, W. Zaremba, A. Szlam, and Y. LeCun, "Spectral Networks and Locally Connected Networks on Graphs," *ArXiv13126203 C*, Dec. 2013.
- [17] D. I. Shuman, S. K. Narang, P. Frossard, A. Ortega, and P. Vandergheynst, "The emerging field of signal processing on graphs: Extending high-dimensional data analysis to networks and other irregular domains," *IEEE Signal Process. Mag.*, vol. 30, no. 3, pp. 83–98, May 2013.
- [18] A. Sandryhaila and J. M. F. Moura, "Discrete Signal Processing on Graphs," *IEEE Trans. Signal Process.*, vol. 61, no. 7, pp. 1644–1656, Apr. 2013.
- [19] T. N. Kipf and M. Welling, "Semi-Supervised Classification with Graph Convolutional Networks," *ArXiv160902907 Cs Stat*, Sep. 2016.
- [20] "How powerful are Graph Convolutional Networks?" [Online]. Available: <http://tkipf.github.io/graph-convolutional-networks/>. [Accessed: 16-Oct-2017].
- [21] D. K. Hammond, P. Vandergheynst, and R. Gribonval, "Wavelets on graphs via spectral graph theory," *Appl. Comput. Harmon. Anal.*, vol. 30, no. 2, pp. 129–150, Mar. 2011.
- [22] "Citi Bike System Data," *Citi Bike NYC*. [Online]. Available: <http://www.citibikenyc.com/system-data>. [Accessed: 16-Oct-2017].
- [23] "Hyperparameter (machine learning)," *Wikipedia*. 12-Oct-2017.
- [24] "TensorFlow," *Wikipedia*. 11-Oct-2017.
- [25] "sklearn.svm.SVR — scikit-learn 0.19.0 documentation." [Online]. Available: <http://scikit-learn.org/stable/modules/generated/sklearn.svm.SVR.html>. [Accessed: 16-Oct-2017].
- [26] L. Lin, Q. Wang, S. Huang, and A. W. Sadek, "On-line prediction of border crossing traffic using an enhanced Spinning Network method," *Transp. Res. Part C Emerg. Technol.*, vol. 43, no. Part 1, pp. 158–173, Jun. 2014.
- [27] L. Lin, Q. Wang, and A. Sadek, "Short-Term Forecasting of Traffic Volume: Evaluating Models based on Multiple Data Sets and Data Diagnosis Measures," *Transp. Res. Rec. J. Transp. Res. Board*, vol. 2392, pp. 40–47, Dec. 2013.
- [28] "sklearn.svm.SVC — scikit-learn 0.19.0 documentation." [Online]. Available: <http://scikit-learn.org/stable/modules/generated/sklearn.svm.SVC.html>. [Accessed: 16-Oct-2017].
- [29] M. Bastian, S. Heymann, and M. Jacomy, "Gephi: An Open Source Software for Exploring and Manipulating Networks," 2009.
- [30] L. Lin, Q. Wang, and A. Sadek, "Data Mining and Complex Network Algorithms for Traffic Accident Analysis," *Transp. Res. Rec. J. Transp. Res. Board*, vol. 2460, pp. 128–136, Dec. 2014.
- [31] V. D. Blondel, J.-L. Guillaume, R. Lambiotte, and E. Lefebvre, "Fast unfolding of communities in large networks," *J. Stat. Mech. Theory Exp.*, vol. 2008, no. 10, p. P10008, Oct. 2008.
- [32] T. Warerker, "New Yorkers use Citi Bike mostly for commuting: study," *Curbed NY*, 15-Mar-2017. [Online]. Available: <https://ny.curbed.com/2017/3/15/14933604/citi-bike-nyu-study-shorter-commute-time>. [Accessed: 16-Oct-2017].